

Stable Control of a Simulated One-Legged Running Robot with Hip and Leg Compliance

Mojtaba Ahmadi and Martin Buehler, *Member, IEEE*

Abstract—We present a control strategy for a simplified model of a one-legged running robot which features compliant elements in series with hip and leg actuators. For this model, proper spring selection and initial conditions result in “passive dynamic” operation close to the desired motion, without any actuation. However, this motion is not stable. Our controller is based on online calculations of the desired passive dynamic motion which is then parametrized in terms of a normalized “locomotion time.” We show in simulation that the proposed controller stabilizes a wide range of velocities and is robust to modeling errors. It also tracks changes in desired robot velocity and remains largely passive despite a fixed set of springs, masses, and inertias. Comparisons of simulated runs with direct hip actuation show 95% hip actuation energy savings at 3 m/s. Such energy savings are critical for the power autonomy of electrically actuated legged robots.

Index Terms—Robotics, legged locomotion, passive dynamics.

I. INTRODUCTION

RESEARCH in dynamically stable legged locomotion aims at understanding the design, dynamics and control of legged machines with the goal of maximizing dexterity, mobility, speed, and efficiency. Progress in this direction has been difficult due to the high dimensionality, the intermittent and under-actuated nature of locomotion, analytically intractable models, and in practice the multitude of constraints on actuator systems. Despite these difficulties the robotics community has been able to produce over the past 15 years several working dynamically stable monopods [1], [2], bipeds [3]–[7] and quadrupeds [8], [9]. The largest contribution to date is the pioneering work of Raibert and coworkers [10] who have built one-, two-, and four-legged hydraulically actuated robots, based on prismatic compliant legs. With their elegant mechanical designs, apparently complex dynamical behavior can be achieved by relatively simple control algorithms.

In order to exploit the newly gained mobility and speed in applications it is imperative to achieve autonomous operations and eliminate the highly constraining power cord. However, power autonomy in dynamic legged robots is an additional constraint on an already challenging design and control problem, and has only recently received attention in the research community. McGeer [1] has built completely

unactuated gravity powered two-legged mechanisms capable of walking down inclines. Such unforced motion of a mechanical system is called its “passive dynamics.” From the very beginning, Raibert’s robots [10] have exploited this principle for the vertical motion which is produced by the spring-mass system formed by the body and the compliant leg. Others [1], [2] and more recently [12] have succeeded in building electrically actuated robots using a similar design for the vertical dynamics.

This principle is at work in nature as well. Many animals are able to reduce the metabolic cost of running considerably by utilizing the elastic properties of muscles, tendons, and bones distributed in their bodies [13] and limbs [14]–[17]. In fact, springs for energy storage are pervasive in nature, and three generic uses of springs in biological systems are discussed by Alexander [18].

In robot running, the use of compliant elements in more than one joint could translate into further energy savings as well. For example, experimental data in [19] showed that the energy consumption for maintaining the leg swing motion amounted to more than 20J per flight phase even at the moderate speed of 1.2 m/s. This is much higher than the stance energy of 5J and constitutes 40% of the total energy requirement for running. This represents an opportunity for major energy savings based on a robot design with a compliant hip, which provides an unforced response—its passive dynamics—close to the desired hip oscillation during running. Raibert and Thompson [20] investigated a one-legged robot with hip compliance. Via simulations and experiments, they showed that proper selection of the initial conditions allows, in principle, operation at any speed. However, the resulting motion is not stable, and the robot will eventually fall.

The control problem of stabilizing robot running with a compliant hip for fore–aft swinging is much more difficult than that for the compliant leg (vertical oscillation) control for three reasons. First, the leg spring is “reset” by a hard-stop to a nominal length at each lift-off. This is not the case for the hip spring. Second, in addition to controlling forward speed during flight via touchdown foot placement and body pitch during stance, the hip motion has to remain close to its passive motion if energy minimization is to be realized. Third, the hip swing motion has to remain closely synchronized with the vertical motion to achieve stable locomotion.

A simplified version of this problem was solved by McGeer [21] for a biped without torso where two legs were connected via a spring. Based on linearized numerical analysis, he proposed local linear control strategies to achieve stable steady speed running. Here, we offer a control algorithm that stabi-

Manuscript received March 20, 1995; revised October 27, 1995. This work was supported in part by an NSERC Research Grant and an FCAR New Researcher Grant held by M. Buehler. The work of M. Ahmadi was supported by the Ministry of Culture and Higher Education of Iran. This paper was recommended for publication by Associate Editor V. Kumar and Editor S. E. Salcudeon upon evaluation of the reviewers’ comments.

The authors are with the Department of Mechanical Engineering, Centre for Intelligent Machines, McGill University, Montréal, QC, Canada, H3A 2A7.

Publisher Item Identifier S 1042-296X(97)01041-0.

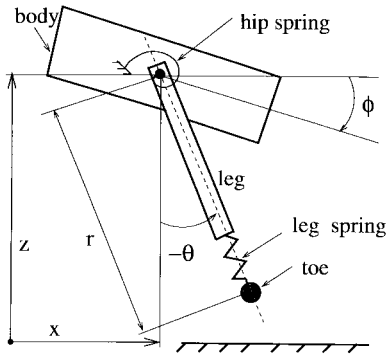


Fig. 1. Model of the simplified monopod. Actuators for control will be in series with each of the springs.

lizes a simplified model of Raibert's one-legged robot with hip and leg compliance, capable of running at a large range of speeds, tracking velocity profiles and capable of dealing with modeling errors. Before proceeding to the solution, we need to clarify the problem.

II. PROBLEM STATEMENT

The most elementary prototype model for the study of dynamically stable locomotion is shown in Fig. 1. This model is based on Raibert's earliest experimental robot [22], and later similar robots [1], [2] built to study the control and energetics of electrically actuated variants. As in [20], we make the simplifying assumptions of negligible frictional losses, zero toe mass, zero spring preload, and a total centre of mass located at the hip joint.

One complete locomotion cycle is illustrated in Fig. 2. It consists of the *flight phase* where the toe does not touch the ground and the robot traverses a ballistic trajectory, and the *stance phase*, where the toe is on the ground and the leg spring is compressed. The beginning of the flight phase and stance phase are termed *lift-off* and *touchdown*, respectively. The instant of maximum and minimum body height are called *apex* and *bottom*. The robot has four degrees of freedom and two actuators, one linear displacement actuator in series with the leg spring and one revolute displacement actuator in series with the hip spring. Since the robot is a variable structure system, we have derived different equations of motion for *flight* and *stance* phases. The spring is massless and the spring force is axial. All the robot variables and parameters are defined in Table I. The equations of motion describe the robot's four degree of freedom during flight,

$$\begin{aligned} \ddot{x} &= 0 \\ \ddot{z} &= -g \\ \ddot{\theta} &= k_h(p_h - \theta + \phi)/J_l \\ \ddot{\phi} &= -k_h(p_h - \theta + \phi)/J_b \end{aligned} \quad (1)$$

and of its three degrees of freedom during stance,

$$\begin{aligned} \ddot{r} &= -g \cos(\theta) + r\dot{\theta}^2 + k_l(r_0 - r + p_l)/m \\ \ddot{\theta} &= [k_h(p_h - \theta + \phi) - 2mr\dot{r}\dot{\theta} + rmg \sin(\theta)]/(J_l + mr^2) \\ \ddot{\phi} &= -k_h(p_h - \theta + \phi)/J_b. \end{aligned} \quad (2)$$

TABLE I
NOMENCLATURE AND NUMERICAL SETTINGS. NUMBERS
IN PARENTHESES REFER TO DEFINING EQUATIONS

g	gravitational acceleration	9.81	m/s^2
J_b	body inertia	2.5	kgm^2
J_l	leg inertia	0.25	kgm^2
k_h	hip spring stiffness	37.8	Nm/rad
k_l	leg spring stiffness	18,120	N/m
m_b	body mass	10	kg
m_l	leg mass	1	kg
m	total mass ($m_b + m_l$)	11	kg
r	leg length (Fig. 1)		m
r_0	maximum leg length	0.7	m
T_f	flight period (6)		s
T_s	stance period (8),(9)		s
T_{step}	step period (4)	0.5	s
x	hip horizontal position (Fig. 1)		m
x_f	foot horizontal distance from hip (Fig. 2)		m
z	hip vertical position (Fig. 1)		m
θ	leg angle w.r.t. vertical (Fig. 1)		rad
ρ	duty factor (11)		
ϕ	body pitch angle (Fig. 1)		rad
ω_h	hip oscillation frequency (3)		rad/s
ω_l	leg oscillation frequency in stance (7)		rad/s

TABLE II
DESCRIPTION OF INDEXES

d	desired value	h	hip	f	flight phase
\cdot	amplitude	l	leg	lo	lift-off
$*$	passive dynamic case	s	stance phase	td	touchdown

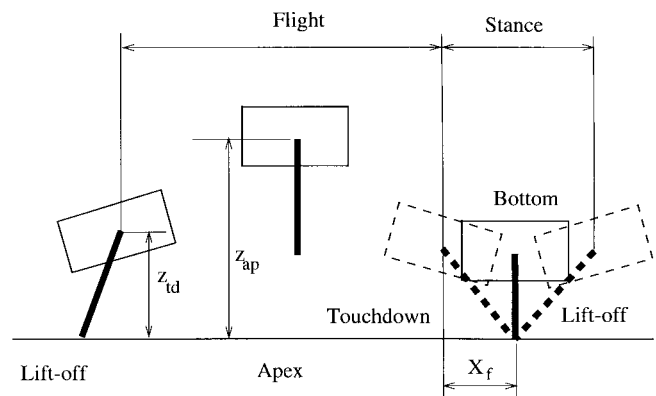


Fig. 2. Locomotion phases during one cycle.

The central idea underlying the use of passive dynamic motion in the hip is illustrated in Fig. 3. If we denote by x_f the horizontal position of the toe with respect to the hip, a completely unforced, frictionless oscillation of the leg and body coupled by the hip spring produces a sinusoidal response. It can now be seen that, with proper initial conditions and coordination with the vertical motion, one can assure

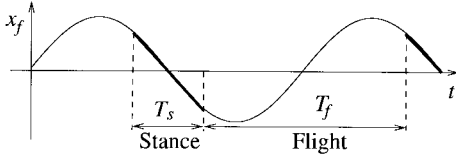


Fig. 3. Foot position with respect to hip with linear approximations of stance phase.

that stance phase occurs during the period of approximately constant slope, equivalent to the robot forward speed. Thus the unforced response can provide for the correct gross hip motion during locomotion.

Two questions must be answered before this idea can be used in practice. Given the robot's design parameters and a desired forward velocity, how to select the passive hip motion and the robot's initial conditions? The answer to this question was given by Raibert and Thompson in [20]. Section III reviews and further elaborates their work in order to prepare for the answer to the second question. This is the central contribution of this paper, addressed in Section IV: How can a legged robot be actively stabilized for a fixed as well as varying velocity while exploiting the passive hip swinging? The answer to this question permits dramatic energy savings which should aid in the development of power autonomous dynamic legged robots.

III. PASSIVE RUNNING

In this section, we derive the initial conditions that result in passive dynamic running, given the robot's design parameters, together with the desired forward speed. To this end we need to examine the dynamics of the hip oscillations in Section III-A, the vertical oscillations in Section III-B, and the effect of their coupling in Section III-C. Section III-D derives initial conditions for purely passive operation, and the resulting performance is presented in Section III-E.

Since the states in this section correspond to the passive dynamic case the variables bear the superscript "*" (e.g., θ^* and ϕ^*). This is necessary to remain consistent with the notation in Section IV where the same variables without "*" correspond to the actual robot states.

A. Hip Oscillation

The natural frequency of the body-leg counter-oscillation of the planar hopper (Fig. 1) can be derived from its equations of motion (1) as

$$\omega_h = \sqrt{\frac{k_h}{J_e}} \quad (3)$$

where $J_e = J_b J_l / (J_b + J_l)$ is the effective moment of inertia for the leg-body counter-oscillation around the hip. Thus the time period for one complete oscillation, the step period, is

$$T_{\text{step}} = \frac{2\pi}{\omega_h}. \quad (4)$$

A symmetric counter-oscillation between leg and body requires that the hip spring is at rest at the initial configuration,

$\theta_0^* = \phi_0^* = 0$. Then any given initial leg speed, $\dot{\theta}_0^*$ is also the leg-speed amplitude, $\dot{\theta}_0^* = \hat{\theta}^*$. Furthermore, the amplitudes of leg speed, $\hat{\theta}^*$, and pitch speed, $\hat{\phi}^*$, are related,

$$\dot{\phi}_0^* = \hat{\phi}^* = -\frac{J_l}{J_b} \hat{\theta}^*. \quad (5)$$

B. Vertical Oscillations

A complete vertical hopping cycle includes stance and flight phases similar to the planar hopper's cycle illustrated in Fig. 2.

Flight: In this phase the purely ballistic robot motion is described by $z(t) = z_{l0} + \dot{z}_{l0}t - gt^2/2$ and

$$z_{\text{ap}} = \frac{\dot{z}_{l0}^2}{2g} + z_{l0}, \quad T_f = \frac{2\dot{z}_{l0}}{g} \quad (6)$$

give the maximum body height (the apex) and the flight duration, respectively, as a function of the vertical liftoff height, z_{l0} , and the vertical lift-off velocity \dot{z}_{l0} .

Stance: Without preload in the spring, the center of mass will follow a sinusoidal motion with a natural frequency:

$$\omega_l = \sqrt{\frac{k_l}{m}}. \quad (7)$$

The equations of motion for stance phase with corresponding initial conditions at touchdown, z_{td} , \dot{z}_{td} , can be written for a simplified vertical mass-spring model $\ddot{z} + \omega_l^2 z = \omega_l^2 z_{td} - g$, with initial conditions $z_0 = z_{td}$, $\dot{z}_0 = \dot{z}_{td}$. The solution of this forced ordinary differential equation including homogeneous and particular solutions is

$$z(t) = z_{td} + \frac{g}{\omega_l^2} \cos(\omega_l t) - 1 + \frac{\dot{z}_{td}}{\omega_l} \sin(\omega_l t).$$

To calculate the stance time T_s , we assume that lift-off and touchdown heights are the same, which is valid for the steady state case. From the condition $z(t = T_s) = z_{td}$ we can now calculate the stance time

$$T_s = \frac{2}{\omega_l} (\pi - \text{Arctan}(-\dot{z}_{td} \omega_l / g)) \quad (8)$$

where \dot{z}_{td} is negative. Assuming that the gravitational forces are small compared to the leg spring forces, this expression can be simplified to

$$T_s \approx \frac{\pi}{\omega_l} \quad (9)$$

which is half of the period of vertical oscillation. This expression for the stance time was used in [20].

C. Leg Spring Stiffening Versus Forward Speed

Accurate knowledge of stance time is important since it is the basis for both the purely passive motion, via the calculation of the initial conditions, and, more critically, for the stabilizing control algorithm proposed in Section IV. If we consider a nominal case with $\dot{z}_{td} = -2$ m/s and $\omega_l = 40.57$ rad/s, (8) gives a stance time of $T_s = \rho T_{\text{step}} = 0.083$ s, versus $T_s = 0.077$ s from (9). This 7.7% error makes (9) undesirable as a basis for control, and in fact leads to rapid failure of the purely passive dynamic running.

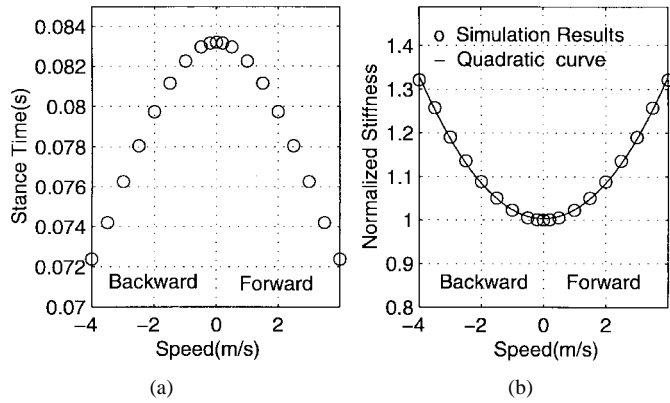


Fig. 4. (a) Simulated stance times and (b) normalized leg stiffness as functions of lift-off horizontal speed at steady state.

However, even (8) is an approximation based on purely vertical hopping. Calculating the exact stance time requires the explicit solution to the robot's equations of motion, a sixth order nonlinear differential equation with boundary values. This, however, is intractable. Instead, we found that we can model the dynamic interaction between the vertical and horizontal dynamics during steady state via modulating the leg's "effective vertical stiffness." That is, as the forward speed increases, the effective leg vertical stiffness increases as well, resulting in a shorter stance time. Neither (8) nor (9) take this effect into account. Therefore, we obtain the relationship between the stance time and forward velocity via simulations at a multitude of speeds (steady states) instead of the above approximate analytical expressions. The resulting relationship is captured in Fig. 4(a), which shows a considerable drop in the stance time as speed increases.

The speed dependent vertical stance oscillation frequency $\omega_l(\dot{x})$ can be found via (8) or (9) starting from the corresponding computed stance time. Based on the computed ω_l an equivalent vertical leg stiffness k_v can be defined via (7),

$$k_v = m\omega_l^2 = m\left(\frac{\pi}{T_s}\right)^2.$$

The computed "normalized stiffness" $k_{\text{norm}} = k_v/k_l$ can be approximated by the second order polynomial, $k_{\text{norm}} = 0.02\dot{x}^2 + 1$ as shown in Fig. 4(b). This matches McMahon's findings [23], that the dimensionless equivalent vertical stiffness of a simple mass-spring system is a quadratic function of forward speed. In Fig. 4, the forward speed at lift-off, \dot{x} , can be replaced by the average stance speed, \bar{x} , defined as

$$\bar{x} = \frac{x_{f,td} - x_{f,lo}}{T_{s,m}} \approx \frac{2}{T_{s,m}}x_{f,td} \quad (10)$$

where $T_{s,m}$ is the measured stance time and the approximation assumes symmetric operation at steady state, $x_{f,lo} = -x_{f,td}$.

D. Selection of Initial Conditions

For purely vertical hopping, the robot design parameters m, J_b, J_l, k_h, k_l determine the hip and leg oscillation frequen-

cies, as well as the duty factor as follows:

$$\begin{aligned} \omega_h &= \frac{2\pi}{T_{\text{step}}} = \sqrt{\frac{k_h}{J_e}}, & \omega_l &= \pi\sqrt{\frac{m}{k_l}} \\ \rho &= \frac{T_s}{T_{\text{step}}} = \frac{\omega_h}{2\omega_l} = 1/2\sqrt{\frac{k_h}{k_l} \frac{m}{J_e}}. \end{aligned} \quad (11)$$

Due to the planar hopper dynamics, these relationships are not correct at nonzero forward speeds. The hip oscillation frequency and the step time is still determined from the robot's design parameters via the first equation above. Then, however, the velocity dependent stance time during steady state passive running is computed, via (9), as

$$T_s = \pi\sqrt{\frac{m}{k_l(0.02\bar{x}^2 + 1)}} \quad (12)$$

from the relationship developed in the previous section. Now the duty factor ρ is determined via $\rho = T_s/T_{\text{step}}$.

The initial conditions are selected to accommodate a desired forward speed \dot{x}_d . Some of the initial conditions, namely $\phi_0^* = 0, \theta_0^* = 0, \dot{z}_0 = 0, x_0 = 0$ are known because we have selected a symmetric oscillatory hip motion. If the initial velocity \dot{x}_0 is under our control, we select $\dot{x}_0 = \dot{x}_d$. If it is not, we select the initial velocity to be the current value of \dot{x} , $\dot{x}_0 = \dot{x}(t_0)$ and rely on the controller (Section IV) to attain the desired velocity \dot{x}_d . Below we will show how to select the initial conditions for the leg speed $\dot{\theta}_0^*$, the body pitch speed $\dot{\phi}_0^*$ and the hip vertical position z_0^* .

Initial Angular Leg Speed: In [20] the desired speed is assumed to be equivalent to the speed at the mid stance $\dot{\theta}_0^* = \dot{x}/r_0$. We observed greatly improved behavior when relying on *average speed*, which also depends on the stance time. This has two reasons. First, the average speed is a better approximation of the sinusoidal curve during stance time. In addition, the dependency on T_s takes some coupling effects between vertical and horizontal dynamics as well as the spring stiffening effect into account. The foot position with respect to the hip is described by

$$x_f = -r_0 \sin \theta^*(t) = -r_0 \sin[\hat{\theta}^* \sin \omega_h t]. \quad (13)$$

Since $\hat{\theta}^* = \dot{\theta}_0^*/\omega_h, \omega_h T_{\text{step}} = 2\pi$, and with (10), (13), the average stance velocity is expressed as

$$\bar{x} = -\frac{2r_0}{T_s} \sin \left[\frac{\dot{\theta}_0^*}{\omega_h} \sin((1-\rho)\pi) \right].$$

By solving for $\dot{\theta}_0^*$ (note again that $\dot{\theta}_0^* = \hat{\theta}^*$) the initial leg angular velocity for passive dynamic running is obtained by

$$\dot{\theta}_0^* = -\frac{\omega_h \arcsin(T_s \bar{x}/2r_0)}{\sin((1-\rho)\pi)}. \quad (14)$$

Initial Body Pitch Speed: At steady state, a zero total angular momentum is assumed during flight. Based on the derivation of $\dot{\theta}_0^*$ in (14) and from (5) we can now calculate the initial body pitch speed as

$$\dot{\phi}_0^* = -\frac{J_l}{J_b} \dot{\theta}_0^*. \quad (15)$$

Initial Hip Vertical Position: At the initial condition the robot is located at “apex” z_{ap} , which can be evaluated by adding the height at touchdown z_{td} and the change of height during the flight phase (see Fig. 2):

$$z_{ap} - z_{td} = \frac{g}{2} \left(\frac{T_f}{2} \right)^2 = \frac{g}{8} (1 - \rho)^2 T_{step}^2. \quad (16)$$

Touchdown occurs at $t_{td} = T_f/2$, hence, the touchdown angle for passive running is

$$\theta_{td}^* = \hat{\theta}^* \sin(\omega_h (1 - \rho) T_{step}/2) = \hat{\theta}^* \sin((1 - \rho)\pi). \quad (17)$$

The touchdown height during passive dynamic running is $z_{td}^* = r_0 \cos \theta_{td}^*$ and finally the initial height can be expressed, using (16) and (17), as

$$z_0^* = z_{ap} = \frac{g}{8} (1 - \rho)^2 T_{step}^2 + r_0 \cos[\hat{\theta}^* \sin((1 - \rho)\pi)]. \quad (18)$$

E. Results

Using the nominal parameters given in Table I, we start the robot with the appropriate initial conditions to obtain completely passive runs. Fig. 5 shows simulation runs for forward speeds of 1, 2, and 3 m/s and confirms that we have successfully calculated precisely the initial conditions to operate this highly unstable dynamical system for a considerable number of cycles. Note that, while any run eventually must fail, the lower the forward speed, the longer the system will run successfully. This is due to the fact that at higher speeds our simplifying assumptions are less accurate, and that small errors lead to failure faster. It can be seen from the data that *only the amplitude of the leg-body oscillation* needs to be modified to accommodate a desired forward speed, based on a fixed set of robot parameters. Thus the hip’s “natural oscillation” would be a good basis to define a desired trajectory for control as well.

IV. CONTROLLED PASSIVE RUNNING

Based on the results of the previous section, we can now select the robot’s initial conditions for passive dynamic operation. However, as we saw above, while this is a good basis for energy efficient running, it does not provide stable operation. Inaccuracies resulting from our simplifying assumptions in calculating the initial conditions, from inaccurate robot parameter estimates, or from external perturbations will result quickly in failure—clearly a stabilizing controller is needed. While our robot with four (flight) and three (stance) degrees of freedom is not controllable in the classical sense via the two inputs, it is possible to stabilize the coupled oscillations of those states by proper periodic forcing.

The task of the controller is threefold. First, it computes the passive trajectory for the current speed of the robot. Second, it adds a feedback velocity error term to modulate the passive trajectory to stabilize a desired forward speed. Third, it modulates the trajectory to accommodate variable speed tracking while still remaining close to the passive trajectory to minimize energy consumption. However, first of all, successful locomotion must be based on robust coupling

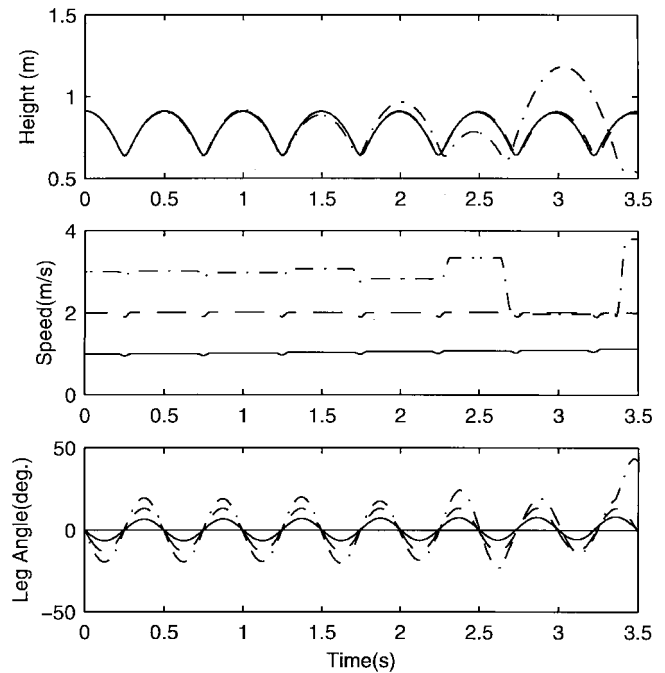


Fig. 5. Even with fixed robot parameters it is possible to run at any speed by changing the leg oscillation amplitude. Shown here are simulation results for 1 m/s (solid), 2 m/s (dashed), and 3 m/s (centered) by using the initial conditions calculated in Section III. All runs are unstable and will eventually fail.

between different degrees of freedom. This is accomplished via a scalar variable termed “locomotion time.” The controller then tracks the trajectories that are all expressed in locomotion times.

A. Locomotion Time

In high degree of freedom underactuated systems like our planar hopper, motion of different joints must be coordinated and often one subsystem may drive others. In our runner, the vertical dynamics determined by gravity during flight and the spring forces during stance act as the “pacemaker,” to which the leg swing must synchronize. For example, when touchdown height is reached, the leg must be at the proper touch down angle, and at bottom (maximum leg compression), it must be vertical (during steady state).

To achieve this synchronization, time is not a suitable parameter because flight or stance times are subject to variations during a run. For example, the desired leg touch down angle must be achieved when the leg touches the ground after a flight phase, if this happens after 0.4 s or 0.8 s. Thus it is desirable to develop a new variable, termed *locomotion time*, which characterizes the dominating dynamics, in our case the vertical motion, independent of the operating conditions (e.g., the hopping height).

A locomotion time should satisfy two conditions. First, it should be a scalar valued function η which maps one flight phase onto the fixed interval $\mathcal{E} = (-1, +1)$ between lift-off $\eta_{lo} = -1$ and touchdown $\eta_{td} = +1$, with $\eta = 0$ at apex. Second, η is an affine function of time. With these two conditions, η becomes a “time-like” parameter suitable

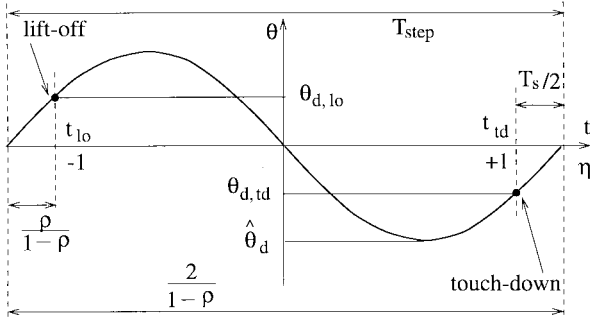


Fig. 6. One complete leg swing oscillation versus time and locomotion time.

for motion planning with synchronization. One such measure during flight time is

$$\eta_1 = \frac{-\dot{z}}{\dot{z}_{lo}}. \quad (19)$$

It is easy to verify that η_1 satisfies the first condition, and compliance with the second condition is also assured since

$$\begin{aligned} \eta_1 &= -\frac{1}{\dot{z}_{lo}} \left(\dot{z}_{lo} - g \left(t + \frac{T_f}{2} \right) \right) \\ &= \frac{g}{\dot{z}_{lo}} \left(t + \frac{T_f}{2} \right) - 1 = \frac{2}{T_f} t. \end{aligned}$$

However, in practice, a measure depending on a single, possibly noisy velocity reading \dot{z}_{lo} , is not desirable. Therefore we use a variant of (19),

$$\eta_f = \frac{-\dot{z}(t)}{\sqrt{E_{\text{vert}}(t)}} \quad (20)$$

where the single lift-off velocity measurement \dot{z}_{lo} is replaced with the square root of the continuous measurement of the vertical total energy $E_{\text{vert}} = 2g(z - z_{lo}) + \dot{z}^2$. This new measure is equivalent to η_1 since at lift-off, the denominator is $\sqrt{E_{\text{vert},lo}} = \dot{z}_{lo}$ and, assuming no energy losses during flight, $E_{\text{vert}} = 0$.

So far, we have not been able to find a locomotion time variable η_s during stance which satisfies the two conditions without requiring an *a priori* knowledge of the stance time T_s . Fortunately, we have already available from the passive dynamics calculations an accurate map between forward velocity and stance time, which we use to obtain the locomotion time during stance

$$\eta_s = \frac{2}{T_s} t \quad (21)$$

and which maps the stance time interval $(-T_s/2, +T_s/2)$ onto the interval $(-1, +1)$. To clarify, Fig. 6 depicts one complete leg swing oscillation both as a function of time as well as locomotion time. In summary, we have now at our disposal a scalar quantity which maps both the stance and flight phases onto a fixed scalar interval and which can now form the basis for control.

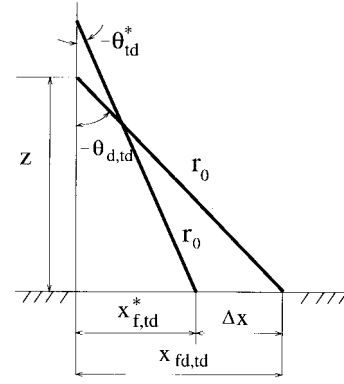


Fig. 7. The leg configuration at touchdown for neutral and deceleration cases.

B. Forward Speed Control During Flight Phase

During flight the leg actuator has no effect, and we are left with only the hip control input, to modulate counter-oscillation of leg and body about the hip axis. Either leg, pitch, or hip angle (angle between the leg and body) can be controlled. We decided to control the leg angle such that forward speed can be affected via selection of the foot placement at touchdown as in [10].

First, given the current forward speed, we obtain the “passive” leg touchdown angle θ_{td}^* , required for passive dynamic operation at that speed from (17). The corresponding passive foot touchdown angle with respect to the hip is $x_{f,td}^* = -r_o \sin \theta_{td}^*$. Forward speed can now be controlled toward the desired one by simply adding a proportional and a derivative error term, to obtain the desired foot touchdown position with respect to the hip,

$$x_{f,td,d} = x_{f,td}^* + \kappa_x(x - x_d) + \kappa_{\dot{x}}(\dot{x} - \dot{x}_d). \quad (22)$$

Fig. 7 illustrates how the correction term affects the foot position and leg angle. A translation of the control law (22) in the desired leg touchdown angle is

$$\theta_{d,td} = -\sin^{-1} \left[-\sin(\theta_{td}^*) + \frac{\kappa_x}{r_o}(x - x_d) + \frac{\kappa_{\dot{x}}}{r_o}(\dot{x} - \dot{x}_d) \right]. \quad (23)$$

The resulting desired amplitude of oscillation $\hat{\theta}_d$, is now determined via the duty cycle, ρ , by

$$\hat{\theta}_d = \frac{\theta_{d,td}}{\sin(\pi(1 - \rho))}. \quad (24)$$

The desired leg angle trajectory can be expressed in the time domain as $\theta_d(t) = \hat{\theta}_d \sin(\omega_n t)$, where $\hat{\theta}_d$ is the desired amplitude of oscillation. Finally, we express this trajectory in the η domain in order to achieve proper synchronization between the leg swing motion and the vertical oscillation,

$$\theta_d(\eta) = \hat{\theta}_d \sin(\pi(1 - \rho)\eta). \quad (25)$$

Fig. 8 shows how the desired path of the leg motion is generated where each block contains the corresponding equation number. Based on the flight dynamics (1) the leg angle is

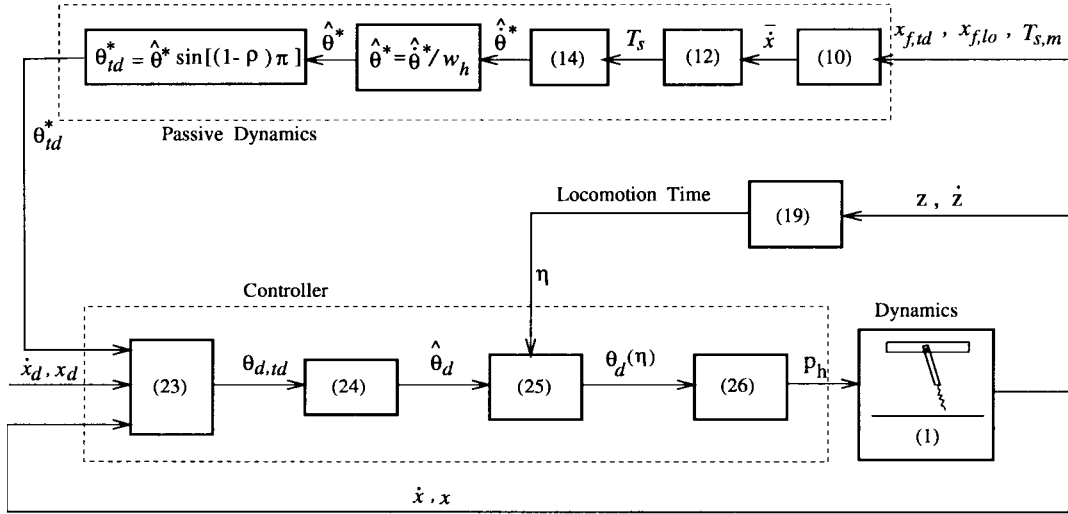


Fig. 8. Flight leg swing controller.

now tracked by recourse to a standard model based inverse dynamic controller of the form:

$$p_h = \frac{J_l}{k_h} (\ddot{\theta}_d + k_v \dot{e}_\theta + k_p e_\theta) + \theta - \phi \quad (26)$$

resulting in the assignable error dynamics $\ddot{e}_\theta + k_v \dot{e}_\theta + k_p e_\theta = 0$, $e_\theta = \theta_d - \theta$. When the steady state error is zero, the actuator displacement p_h will also be zero.

C. Control During Stance Phase

During stance, the hip actuator controls the body's pitch angle ϕ . At the same time, the leg actuator controls the hopping height by introducing a displacement at bottom p_l .

Pitch Angle Control: The controller again uses inverse dynamics to track the desired pitch trajectory $\phi_d = \hat{\phi}_d \sin(\omega_h t)$. The amplitude of the body oscillation $\hat{\phi}_0$ is determined from the fact that the total angular momentum of the robot is to be kept zero, as determined by the passive dynamic operation. Therefore the desired pitch oscillation amplitude is proportional to the leg angle amplitude $\hat{\phi}_d = -J_b/J_l \hat{\theta}_d$. Based on the hopper's equation of motion during the stance phase (2) the controller takes the form

$$p_h = -\frac{J_b}{k_h} (\ddot{\phi}_d + k_v \dot{e}_\phi + k_p e_\phi) + \theta - \phi \quad (27)$$

where $e_\phi = \phi_d - \phi$. The desired pitch angle at touchdown ($\eta_s = 1$) is $\phi_{d,td}$, and the same magnitude but negative angle is expected at lift-off ($\eta_s = -1$). Thus $\phi_d(\eta_s)$ is found by relating η_s and t in a similar fashion as above, by changing the time interval from $T_f/2$ to $T_s/2$:

$$\begin{aligned} \phi_d &= \hat{\phi}_d \sin(\omega_h t) = \hat{\phi}_d \sin\left(\frac{2\pi}{T_{\text{step}}} \frac{T_s}{2} \eta_s\right) \\ &= \hat{\phi}_d \sin(\pi \rho \eta_s). \end{aligned} \quad (28)$$

Hopping Height Control: The hopping height is controlled by a proportional controller that is active intermittently during each decompression phase, $p_l = k_z(z_{ap} - z_{\max})$, where z_{ap} is the desired body apex height obtained from (18) and z_{\max} is the last hopping height.

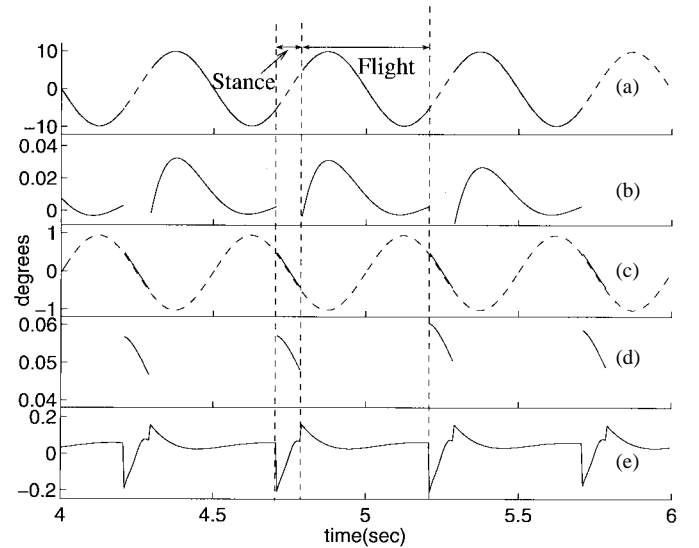


Fig. 9. Simulation results of controlled compliant running at 1.5 m/s. Panel (a) shows the actual and desired leg angle, (b) leg angle error, (c) actual and desired pitch angle, (d) pitch angle error, and (e) hip actuator displacement (Desired: dashed; Actual: solid).

D. Results

The effectiveness of our control strategy is shown at steady state, while tracking, and in the face of modeling errors.

Steady State: Fig. 9 demonstrates that the robot leg (during flight) and body pitch (during stance) errors are very small. This shows the ability of the controller to operate and stabilize the robot around the passive dynamic trajectories. At the same time the actuator effort, shown in the lower trace, is very small and remains within $\pm 0.2^\circ$. To validate our main objective of reducing the energy requirements compared to direct actuation, we have run both compliant and direct actuation simulations with different desired speeds. By setting the spring stiffness to a high value, our approach can be applied to control a directly actuated hip as well. Fig. 10 shows the total hip energy consumed in six seconds and verifies that dramatic energy savings of approximately 95% are achievable when exploiting

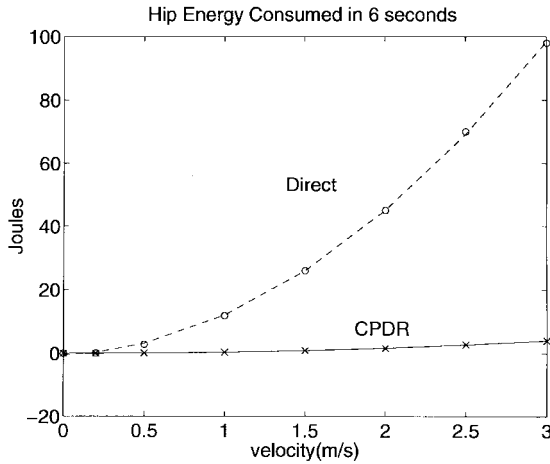


Fig. 10. Energy consumption in the hip actuator. Comparison between compliant and direct actuation. Controlled passive dynamic running (CPDR) saves about 95% of the hip energy required by direct actuation.

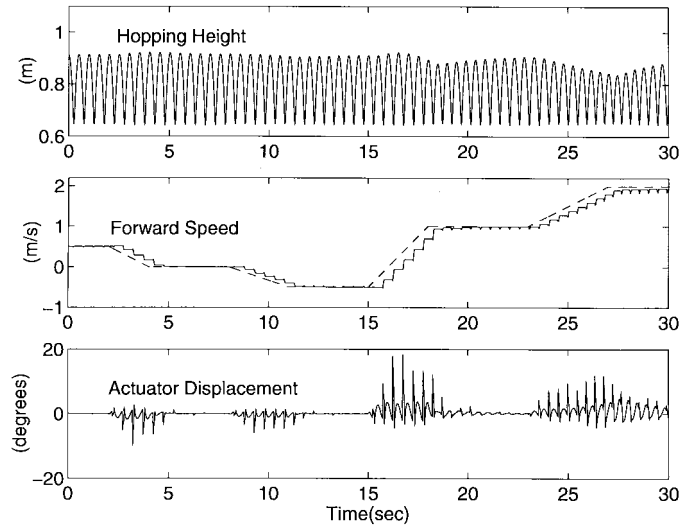


Fig. 12. Hopping height, velocity variation, and hip actuator displacement for velocity tracking.

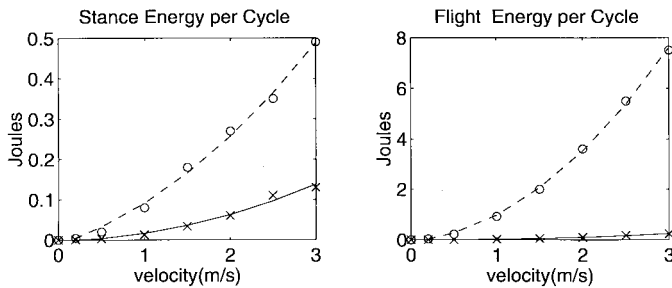


Fig. 11. In direct actuation, 90% of the energy is expended during flight phase, just to swing the leg. Virtually all of this energy can be saved by relying on a passive oscillation based on a hip compliance (CPDR = controlled passive dynamic running).

passive dynamics. Fig. 11 illustrates why the hip compliance is so effective: In direct actuation, 90% of the energy is expended during flight phase, just to swing the leg. Virtually all of this energy can be saved by relying on a passive oscillation based on a hip compliance.

Tracking: Fig. 12 shows simulation runs with ramp changes in commanded speed to demonstrate robust tracking performance of the controller, even though it was designed based on steady state operation. In fact, the same controller successfully tracks step inputs up to 2 m/s, provided that large actuator displacements can be accommodated.

Robustness: The robustness of the controller is investigated for relatively large and cumulative modeling errors, as shown in Fig. 13. First, as the robot runs at a steady state velocity of 1 m/s, we introduce a modeling error of 20% in the robot’s body mass. Next, an *additional* (simultaneous) error of 20% in body inertia, and finally an *additional* error in spring stiffness of 20% is introduced. The controller shows a high degree of robustness to these large modeling errors: It maintains stability, and the error in forward velocity is less than 10%. The energy consumption increases from 0.01J to 0.2J.

The controller’s strong robustness is a good indication that it might also work well in practice. Practical implementations would have to deal with actuator limitations as well, which we have not yet considered. These may decrease but lengthen the

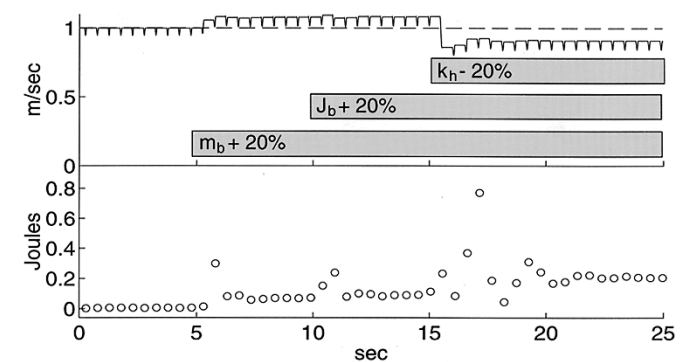


Fig. 13. Robustness tests. Effect of modeling errors on forward speed and on the hip energy consumption per cycle.

transient energy peaks shown in Fig. 13. It is important to note that the role of the inverse dynamic controller is a minor one, namely tracking the reference trajectories specified on-line by our trajectory planner. The key to the success of the approach is the robust synchronization between vertical and leg-swing motion via the locomotion time, and the trajectory planning for the leg swing motion based on the compliant passive dynamics. The results are stable and robust compliant running, small actuator displacements, and low energy consumption.

V. CONCLUSION

We have presented a new control strategy for dynamically stable legged locomotion with compliant elements. It exploits the underlying passive dynamic operation for minimum energy consumption while still ensuring stable and robust control and forward speed tracking. By using the passive motion trajectory of the swinging leg at the current robot speed as the basis for motion planning, stability can be achieved by recourse to standard model based control techniques.

The method was successful in simulation, but still needs to be verified experimentally. Implementations will be aided by the robustness of the controller to large desired speed vari-

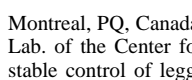
ations and unmodeled dynamics—the controller is based on many simplifying assumptions, while the simulation included the full planar dynamics and a compliant ground model. To implement this method, we will need a more complete robot model for the passive dynamic trajectory calculations and analyze the effect of friction and nonlinearity of the springs. In the presence of losses in physical systems, the energy savings between direct and compliant actuation might be less than reported here. However, we still expect to see major energy savings which would contribute greatly toward autonomy and reduced cost by down-sizing actuator power requirements. Similar energy savings could be achieved in multilegged robots by exploiting the passive compound oscillations during trotting, pacing and bounding gaits.

REFERENCES

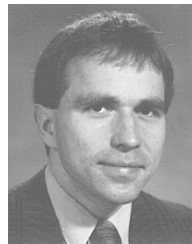
- [1] K. V. Papanatiou, "Electromechanical design for an electrically powered, actively balanced one leg planar robot," in *Proc. IEEE/RSJ Conf. Intelligent Systems and Robots*, Osaka, Japan, 1991, pp. 1553–1560.
- [2] P. Gregorio, M. Ahmadi, and M. Buehler, "Experiments with an electrically actuated planar hopping robot," in *Experimental Robotics III*, T. Yoshikawa and F. Miyazaki, Eds. New York: Springer-Verlag, 1994, pp. 269–281.
- [3] H. Miura and I. Shimoyama, "Dynamic walk of a biped," *Int. J. Robot. Res.*, vol. 3, no. 2, pp. 60–74, 1984.
- [4] A. Takahashi, M. Ishida, M. Yamazaki, and I. Kato, "Realization of dynamic walking by the biped walking robot WL-10RD," in *Proc. Int. Conf. Advanced Robotics*, 1985, pp. 459–466.
- [5] J. Furusho and M. Masubuchi, "Control of a dynamical biped locomotion system for steady walking," *ASME J. Dynamics Syst., Meas., and Contr.*, vol. 108, pp. 111–118, June 1986.
- [6] S. Kajita, K. Tani, and A. Kobayashi, "Dynamic walk control of a biped robot along the potential energy conserving orbit," in *IEEE Int. Workshop Intelligent Robots and Systems*, 1990, pp. 789–794.
- [7] A. Sano and J. Furusho, "Realization of natural dynamic walking using the angular momentum information," in *Proc. IEEE Int. Conf. Robotics and Automation*, 1990, pp. 1476–1481.
- [8] H. Miura, I. Shimoyama, M. Mitsuishi, and H. Kimura, "Dynamical walk of quadruped robot (Collie-1)," in *Int. Symp. Robotics Research*, H. Hanafusa and H. Inoue, Eds. Cambridge, MA: MIT Press, 1985, pp. 317–324.
- [9] Y. Sakakibara, K. Kan, Y. Hosoda, M. Hattori, and M. Fujie, "Foot trajectory for a quadruped walking machine," in *IEEE Int. Workshop Intelligent Robots and Systems*, 1990, pp. 315–322.
- [10] M. H. Raibert, *Legged Robots That Balance*. Cambridge, MA: MIT Press, 1986.
- [11] T. McGeer, "Passive dynamic walking," *Int. J. Robot. Res.*, vol. 9, no. 2, pp. 62–82, 1990.
- [12] A. Lebaudy, J. Prosser, and M. Kam, "Control algorithms for a vertically-constrained one-legged hopping machine," in *Proc. IEEE Int. Conf. Decision and Control*, 1993, pp. 2688–2693.
- [13] R. McN. Alexander, N. J. Dimery, and R. F. Ker, "Elastic structures in the back and their role in galloping in some mammals," *J. Zoology (London)*, vol. 207, pp. 467–482, 1985.
- [14] N. J. Dimery, R. McN. Alexander, and R. F. Ker, "Elastic extension of leg tendons in the locomotion of horses," *J. Zoology (London)*, vol. 210, pp. 415–425, 1986.
- [15] R. McN. Alexander, G. M. O. Maloij, R. F. Ker, A. S. Jayes, and C. N. Warui, "The role of tendon elasticity in the locomotion of the camel," *J. Zoology (London)*, vol. 198, pp. 293–313, 1982.
- [16] G. A. Cavagna, H. Thys, and A. Zamboni, "The source of external work in level walking and running," *J. Physiol.*, vol. 262, pp. 639–657, 1976.
- [17] T. A. McMahon, "The role of compliance in mammalian running gaits," *J. Exp. Biol.*, vol. 115, pp. 263–282, 1985.
- [18] R. McN. Alexander, "Three uses for springs in legged locomotion," *Int. J. Robot. Res.*, vol. 9, no. 2, pp. 53–61, 1990.
- [19] P. Gregorio, "Design, control and energy minimization strategies for an electrically actuated legged robot," M.Eng. thesis, McGill Univ., Montreal, PQ, Canada, Aug 1994.
- [20] M. H. Raibert and C. M. Thompson, "Passive dynamic running," in *Experimental Robotics I*, V. Hayward and O. Khatib, Eds. New York: Springer-Verlag, 1989, pp. 74–83.
- [21] T. McGeer, "Passive bipedal running," Tech Rep. IS-TR-89-02, Simon Fraser Univ., Centre for Syst. Sci., Apr. 1989.
- [22] M. H. Raibert, "Dynamic stability and resonance in a one-legged hopping machine," *4th Symp. Theory and Practice of Robots and Manipulators*, 1981, pp. 491–497.
- [23] T. A. McMahon and G. C. Cheng, "The mechanics of running: How does stiffness couple with speed?" *J. Biomechanics*, vol. 23, pp. 65–78, 1990.



Mojtaba Ahmadi was born in Tehran, Iran. He received the B.S. degree from Sharif University of Technology in 1988 and the M.S. degree in 1992 from The University of Tehran, Iran, both in mechanical engineering.



He has worked on the simulation of mechanical systems at the Industrial Research Institute, Tehran, Iran, and has been a technical consultant to "Ports and Shipping Organization," Iran. Since 1993, he has been a Ph.D. student with the Department of Mechanical Engineering at McGill University, Montreal, PQ, Canada, and a research assistant with the Ambulatory Robotics Lab. of the Center for Intelligent Machines. He is currently working on the stable control of legged systems with joint compliance.



Martin Buehler (S'85–M'90) was born in Lahr, Germany, in 1961. He holds the M.Sc. degree and the Ph.D. degree in electrical engineering from Yale University, New Haven, CT, in 1985 and 1990, respectively.

Until 1991, he was working as a post-Doctoral associate in the LegLab at MIT's Artificial Intelligence Lab. Since 1991, he has been an Assistant Professor with the Department of Mechanical Engineering at McGill University, Montreal, PQ, Canada. His research interests are in the areas of robot manipulation and legged locomotion. He is currently the Project Leader for "Machine Sensing and Actuation I," an IRIS/PREARN project of the Federal Network of Centres of Excellence.

Dr. Buehler held a junior Industrial Research Chair from 1991–1995 and is a Scholar of the Canadian Institute for Advanced Research.